Effect of Energy Metabolism on Protein Motility in the Bacterial Outer Membrane

Tabita Winther,[†] Lei Xu,[†] Kirstine Berg-Sørensen,[‡] Stanley Brown,[§] and Lene B. Oddershede[†*]
[†]The Niels Bohr Institute, University of Copenhagen, Copenhagen, Denmark; [‡]Department of Physics, Technical University of Denmark, Lyngby, Denmark; and [§]Department of Biology, University of Copenhagen, Copenhagen, Denmark

ABSTRACT We demonstrate the energy dependence of the motion of a porin, the λ-receptor, in the outer membrane of living *Escherichia coli* by single molecule investigations. By poisoning the bacteria with arsenate and azide, the bacterial energy metabolism was stopped. The motility of individual λ-receptors significantly and rapidly decreased upon energy depletion. We suggest two different causes for the ceased motility upon comprised energy metabolism: One possible cause is that the cell uses energy to actively wiggle its proteins, this energy being one order-of-magnitude larger than thermal energy. Another possible cause is an induced change in the connection between the λ-receptor and the membrane structure, for instance by a stiffening of part of the membrane structure. Treatment of the cells with ampicillin, which directly targets the bacterial cell wall by inhibiting cross-linking of the peptidoglycan layer, had an effect similar to energy depletion and the motility of the λ-receptor significantly decreased. Since the λ-receptor is closely linked to the peptidoglycan layer, we propose that λ-receptor motility is directly coupled to the constant and dynamic energy-consuming reconstruction of the peptidoglycan layer. The result of this motion could be to facilitate transport of maltose-dextrins through the porin.

INTRODUCTION

Insight into membrane protein motility is important for the understanding of nutrient uptake and regulatory mechanisms, and for understanding the action of antibiotics in procaryotes. There have been numerous investigations of mobility of proteins in the membranes of eukaryotic cells (1–3), but few on the mobility of proteins in the outer membranes of living prokaryotic cells (4–7). Membrane proteins cannot be viewed as isolated structures; their function is deeply dependent on their environment—i.e., the membrane—as well as energy availability and regulatory mechanisms. For lipid bilayers, it has been theoretically predicted that there should be a connection between the energetic activation of proteins and the membrane compartmentalization (8). In addition, the spatial organization and oligomerization of bacteriorhodopsin embedded in artificial membranes has been shown to depend on photoactivation; at particular protein concentrations, a decrease in protein motility was observed upon photoactivation (9). In this article, we further investigate the possible influence on energy availability on protein motility in the membrane of a living *Escherichia coli*.

The outer membrane of Gram-negative bacteria is an asymmetric structure that functions as a permeability barrier allowing for transport predominantly through specific pores and channels (10). The main components of the outer part of the cell wall are the outer leaflet consisting of lipopolysaccarides; the inner leaflet consisting of phospholipids; and the peptidoglycan layer, a strong structure that enables the bacterium to maintain a large osmotic pressure gradient across the cell wall. The λ-receptor is an integral outer membrane protein, which is responsible for the transport of maltodextrins across the outer membrane (11), and it is proposed to be attached to the peptidoglycan layer (12). As it is the receptor for bacteriophage lambda, it has been studied for more than 40 years and the regulation as well as the genetics of the receptor is well understood. There can easily be thousands of λ-receptors present in the outer membrane, and they have been reported to have a homogeneous distribution in cells at times significantly after induction (13,14). However, recently they have also been reported to be expressed in a helical pattern (6), a pattern also followed by other types of membrane proteins (15). In vivo studies of the mobility of a single λ-receptor consistently found that the λ-receptor performs a ''wiggling motion'', which can be characterized as a confined diffusional motion within the outer membrane (4–6).

In this work, we examined the role of energy metabolism on the motility of a single λ-receptor in the outer membrane of *E. coli*. In metabolically competent cells, we utilized an inefficient biotinylation scheme, which ensured single molecule observation and monitored the motion of a single λ-receptor using both beads and quantum dots, thus clarifying a literature controversy regarding the magnitude of the confined diffusion (4,6).

To study the effect of a comprised energy metabolism, we monitored the motility of the same receptor both before and after energy depletion of the cells by arsenate, which stops adenosine triphosphate (ATP) synthesis, and azide, which stops electron transport. This treatment gave rise to a significant and rapid decrease of motility. Hence, the motility of a λ-receptor in an energetically competent cell is not purely caused by thermal motion. In addition, there is an active

Submitted March 19, 2009, and accepted for publication June 15, 2009.

*Correspondence: oddershede@nbi.dk

Editor: Michael Edidin.

0006-3495/09/09/1305/8 $2.00

doi: 10.1016/j.bpj.2009.06.027

contribution; this contribution is approximately one-order-of-magnitude larger than the thermal energy. We invoke a model with two possible causes for the observed change in λ-receptor motility upon energy depletion: one cause could be that a metabolically competent cell actively spends energy, which results in a wiggling of its λ-receptors, and another possible cause could be a change in the membrane structure caused by energy depletion. To pinpoint the biological cause of the observed effects, we treated the cells with ampicillin, an inhibitor of peptidoglycan crosslinking. The effect of ampicillin was to efficiently stop the motion of the receptor. Based on these observations, we propose that the λ-receptor through its firm connection to the peptidoglycan layer uses the energy-dependent dynamic reconstruction of this layer to perform a wiggling motion.

MATERIALS AND METHODS

Bacterial strains

The strains used were derived from S2188 (16), an *E. coli* K12 strain which has a deletion in the *lamB* gene. A plasmid harboring the biotinylated λ-receptor was then inserted into strain pLO16, which was used throughout this study; for a more detailed description, see Oddershede et al. (4), where it is also proven that the efficiency of the biotinylation is very low—on average less than one receptor per bacterium is biotinylated. This greatly reduces the risk of having a bead attached to more than one receptor simultaneously.

Growth and preparation of bacteria

Single colonies of bacteria were grown at 37°C on YT agar plates (17) supplemented with 25 μg/mL chloramphenicol. A single colony was suspended in M63 salts (18) containing 1 μg/mL B1, 25 μg/mL chloramphenicol, 0.1% casein hydrolysate, and 0.2% glycerol. The bacteria were grown overnight in a shaking water bath at 37°C. Thereafter 0.1 mL of suspended bacteria was diluted into 3 mL fresh MOPS media (19), where they were grown until log-phase, still at 37°C. MOPS was chosen as the growth medium, as it can be phosphate-free and therefore is well suited as medium also during poisoning with arsenate. The poisoning has to be carried out in a phosphate-free solution, because the metabolic inhibition by arsenate is caused by its resembling the phosphate group that participates in the energy transfer. After reaching log-phase, isopropyltriogalactoside (IPTG) was added to a final concentration of 0.5 mM, and the bacteria were grown for an additional half-hour. IPTG is used to induce the expression of the λ-receptor. One milliliter of this culture was then centrifuged for 5 min at 1673 × *g* and the pellet was resuspended in buffer. The buffer used throughout the experiments was a KCl-potassium phosphate (10 mM potassium phosphate, 0.1 M KCl, pH 7) buffer. The beads used were streptavidin-coated polystyrene spheres from Bangs Laboratories (Fishers, IN), most often with a diameter of 0.44 μm. The remaining parts of the preparation procedure were performed at room temperature (22°C): The beads were washed by suspension in Millipore water and thereafter centrifuging them at 1673 × *g* for 5 min (Millipore, Billerica, MA). The supernatant was discarded and the beads resuspended in buffer and sonicated for at least 15 min to disrupt aggregates. To study the bacteria in the microscope, perfusion chambers were made. On a poly-L-lysine coated coverslip, two pieces of double sticky tape were put together to form a chamber and another coverslip was then attached as the lid of the chamber. To allow the bacteria to attach to the poly-L-lysine coated surface, the bacteria were incubated at room temperature for 20 min. Heparin (12.5 mg/ml) was perfused into the chambers and incubated at room temperature for 15 min. The heparin layer passivates the charges of the poly-L-lysin, which thereby minimizes the attraction between the poly-L-lysin coated coverslip and the streptavidin-coated beads (4). The chambers were then washed four times with buffer, after which the washed streptavidin-coated beads were flushed in and left to adhere to biotinylated receptors for 15 min, still at room temperature. To remove excess beads, the chambers were then washed until they appeared clear. They were washed with MOPS media with the difference from the MOPS mentioned above that the glycerol was replaced with glucose. Glucose was used to support anaerobic growth in the closed chambers. The chambers were inverted and stored over a water bath at 5°C until use.

Optical tweezers setup

The optical tweezers setup is based on a Spectra-Physics Millennia Nd:YVO_4 laser (Newport, Irvine, CA) implemented in an inverted Leica DM IRBE microscope (Leica, Solms, Germany). The laser light is tightly focused by a Leica objective (100× oil NA 1.4 PL APO); after passage of the sample, the light is collected by an oil immersion condenser and imaged onto a photodiode. Two types of photodiodes were used: one was a quadrant photodiode (model No. S5981 Si-PIN ; Hamamatsu, Hamamatsu City, Japan) and the other a position-sensitive diode (model No. DL100-7PCBA3; Pacific Silicon Sensors, Westlake Village, CA). With this setup, we can measure forces and distances in the piconewton and nanometer regimes with a time resolution of MHz. A detailed description of the setup can be found in Oddershede et al. (20). The duration of an optical tweezers measurement is approximately seconds, and the sampling rate was 22,000 Hz, giving a temporal resolution of 46 μs. To ensure that the mobility of exactly the same receptor was recorded before and after poisoning the entire experiment was video recorded using a model No. XC-ES50 charge-coupled device (CCD) camera (Sony, Tokyo, Japan). The experiments, which included visualization of individual quantum dots, were performed in a Leica SP5 confocal microscope equipped with an sXon+ cooled EMCCD camera (Andor, Belfast, Northern Ireland) and a normal fiber-coupled Leica Hg excitation source. The laser power delivered at the sample was ~10 mW and the total exposure time was approximately a few seconds. At such low laser power and low exposure time, no physiological damage has been detected on optically trapped bacterial species (21).

Experiments with beads as markers

The first step in the experimental procedure was to trap a free bead and perform a force calibration of a bead at the same height as a bead attached to a λ-receptor (4). Next, we found a bead attached to a λ-receptor, this attachment being characterized by a wiggling motion of the bead (4). If a bead is not specifically attached, it does not perform this wiggling motion (4), and it can be pulled away by an optical trap, thus creating a tether consisting of outer membrane material (22). In this investigation, we centered the optical trap on a bead that was specifically attached to a λ-receptor and recorded a time series of its motion using the photodiode and custom-made LabVIEW programs (National Instruments, Austin, TX).

Energy depletion

After the steps described in the above paragraph, the liquid in the perfusion chambers was exchanged by flushing 20 μL of an arsenate and azide poison mixture through the chamber five times. The poison mixture consisted of phosphate free MOPS supplemented with 20 mM NaN_3 and 1 mM KH_2AsO_4. This procedure was repeated after a waiting period of roughly 10 min. This tedious procedure of poisoning ensures that all the liquid in the perfusion chamber is replaced with the poisonous liquid, and that the poison has time to affect the cells. Another time series of the positions visited by the same λ-receptor was recorded after poisoning.

Ampicillin

In the experiments with ampicillin, the cells were grown in M63 as described above. After reaching log-phase, the M63-IPTG solution was supplemented

by 100 μg/mL ampicillin and the cells were grown for at least 1 h with ampicillin present. Then the remaining part of the procedure outlined in Growth and Preparation of Bacteria was conducted, but with the modification that all solutions contained 12% sucrose. The sucrose was included to osmotically stabilize cells with compromised cell walls.

Three types of experiments were performed:

1. An experiment in which ampicillin was present during both growth and measurement.
2. An experiment in which ampicillin was present during growth, but not during measurement (the measurement procedure was performed in M63).
3. A control experiment in which ampicillin was not present during either growth or measurement, but everything else was the same as for cases 1 and 2.

Experiments with quantum dots as markers

The preparation of these samples was as described above in Growth and Preparation of Bacteria until the point where the beads were added except the bacteria were grown in M63 media throughout the entire procedure, the IPTG concentration was raised to 1 mM, and we attached quantum dots instead of beads. The streptavidin-coated CdSe quantum dots (Invitrogen, Carlsbad, CA) with emission wavelength 655 nm, outer diameter ~15 nm, were diluted 1:10,000 into the growth media (M63), and after addition of 10 μL of the quantum dot solution to the samples, they were sealed. The sample was incubated for 30 min to allow the quantum dots to attach to the receptor before the experiment was initiated. The motion of the quantum dot was observed using an EMCCD camera, taking 50 s time series with a repetition rate of 10 Hz. All frames were overlaid in a stack and for each pixel, the brightest pixel value was chosen for a final, summarized picture. This final picture provided an overview of the total excursions of the quantum dot during the 50 s. The pixels that were not visited appeared dark, whereas those visited appeared brighter. Each pixel corresponded to 25 nm. We only used quantum dots to visualize lambda receptors on metabolically competent bacteria.

Data analysis

The optical tweezers exert a harmonic force on the trapped bead, $F = -\kappa(x_{\text{bead}} - x_{\text{trap}})$, where κ is denoted the spring constant of the optical trap, x_{bead} is the position of the bead, and x_{trap} is the equilibrium position of the optical trap. Similar equations exist for the two orthogonal directions, but as we have chosen only to analyze the receptors that sit on top of the bacteria seen from the microscope's point of view, and since the motion of a λ-receptor is isotropic in the lateral directions (4), it suffices to consider only the x direction in the following analysis. The time series of the bead's motion is measured in Volts by the photodiodes, and is easily converted to meters, e.g., using the procedures written in Oddershede et al. (20). When performing this calibration procedure it is important to account for aliasing and possible filtering by the photodiode and other filters present and we did so using the MATLAB programs described in Hansen et al. (23).

The bead and the protein are joined through a biotin-streptavidin linkage, which is described as a harmonic spring with spring constant κ_{bs}. The potential felt by the protein in the membrane is also well described by a harmonic potential (4), with spring constant κ_{cw}. This spring constant describes the connection to the membrane structure, and an alternation of the cell wall properties would appear in our model as a change in κ_{cw}. The protein also feels some frictional force from the membrane, the friction coefficient being denoted γ_{prot}. Finally, both the bead and the protein are subject to stochastic forces due to the random bombardment by solvent molecules. These stochastic forces are denoted F_{bead} and F_{prot}, and are assumed to have the properties of white noise, i.e., vanishing expectation value and δ-function autocorrelations. F_{bead} and F_{prot} vary with time and temperature, T. The above definitions, as well as the following two coupled equations of motion for, respectively, the bead and the protein, are identical to those outlined in Oddershede et al. (4):

$$M_{\text{bead}}\ddot{x}_{\text{bead}} = -\kappa\left(x_{\text{bead}} - x_{\text{trap}}\right) + \kappa_{\text{bs}}\left(x_{\text{prot}} - x_{\text{bead}}\right) - \gamma_{\text{bead}}\dot{x}_{\text{bead}} + F_{\text{bead}}, \quad (1)$$

$$M_{\text{prot}}\ddot{x}_{\text{prot}} = -\kappa_{\text{cw}}\left(x_{\text{prot}} - x_{\text{cw}}\right) - \kappa_{\text{bs}}\left(x_{\text{prot}} - x_{\text{bead}}\right) - \gamma_{\text{prot}}\dot{x}_{\text{prot}} + F_{\text{prot}}. \quad (2)$$

Here, M_{bead} and M_{prot} are the masses of bead and protein.

Using this model and typical data sets, it turns out that the total spring constant felt by the bead is given by $\kappa_{\text{tot}} = \kappa + \kappa_{\text{cw}}$ (4). When a measurement is done with the optical tweezers system, one obtains a time series of the positions visited by the bead. The corresponding histogram is well described by a Gaussian distribution with standard deviation σ,

$$\sigma^2 = \frac{k_{\text{B}}T}{\kappa + \kappa_{\text{cw}}}. \quad (3)$$

From this expression and the determination of κ from calibration, κ_{cw} can be found. Subsequently, the standard deviation of the positions visited by the protein, σ_λ, can be found as

$$\sigma_\lambda^2 = \frac{k_{\text{B}}T}{\kappa_{\text{cw}}}. \quad (4)$$

Experimentally, a narrowing of the position histogram, the width of which is described by σ_λ, is observed upon energy depletion. Thus, Eq. 4 suggests two interpretations of this narrowing: either T decreases or κ_{cw} increases. These two interpretations are modeled as A or B in the following.

Effect of energy depletion

We propose two ways of modeling the effect of energy depletion.

Model A

We assume that the λ-receptor is actively moved, made to wiggle in a metabolically competent cell. In other words, its total energy is a sum of two terms—one originating from the thermal motion, the other from an active motion (where the cell spends energy to perform this motion):

$$E_{\text{tot}} = E_{\text{thermal}} + E_{\text{active}}. \quad (5)$$

Model A is implemented in Eqs. 1 and 2 by using an artificial temperature, T_{bac}, to describe the total energy: $E_{\text{tot}} = \frac{1}{2}k_{\text{B}}T_{\text{bac}}$. T_{bac} is then put into Eq. 2 in the stochastic force term. Hence, in the fitting routines, T_{bac} is allowed to vary and all other parameters are kept fixed while comparing datasets from metabolically competent cells to energy depleted cells. Model A is illustrated in Fig. 1, where a ''pickup truck'' is drawn as the active mover of the λ-receptor before energy depletion.

Model B

We assume that the effect of energy depletion predominantly alters the membrane structure and that this gives rise to a change of κ_{cw}. Hence, in the fitting routines, κ_{cw} is allowed to vary and all other parameters, including temperature, are kept fixed while comparing datasets from metabolically competent cells to energy depleted cells. Model B is also illustrated in Fig. 1 where the change in the cell wall is drawn as an aggregation of membrane proteins around the λ-receptor and as a stiffening of the attachment of the λ-receptor to the peptidoglycan layer.

Both models

In Eqs. 1 and 2, the inertial terms are significantly smaller than the other terms and may be neglected. Thus simplified, Eqs. 1 and 2 are Fourier-transformed and the power spectrum of the position of the bead, $P_{\text{bead}}(f)$, is derived as

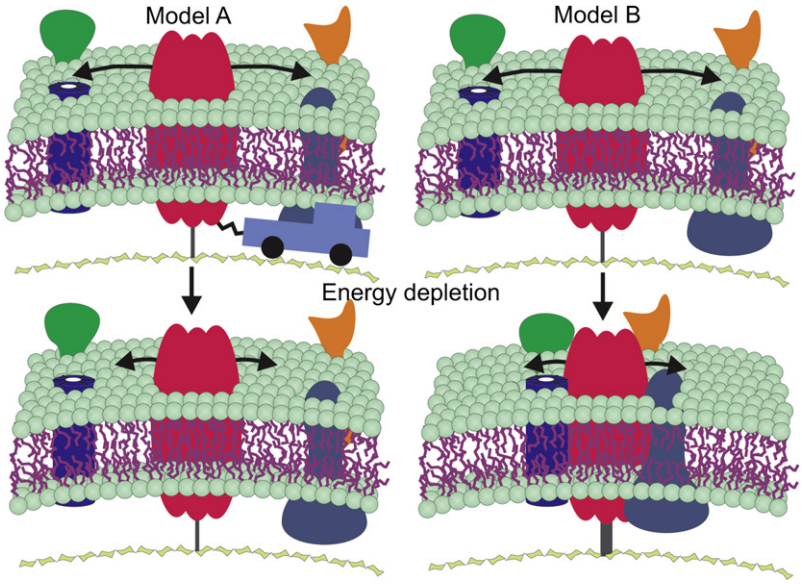

FIGURE 1 An illustration of models A and B for the effect of energy depletion. The λ-receptor is a trimer located in the outer membrane of *E. coli* bacteria; it is assumed to connect to the peptidoglycan layer (12). In model A, the λ-receptor in a metabolically competent cell is assumed to be actively moved; the cell spends energy to wiggle the λ-receptor. This is illustrated by the "pickup truck" moving the protein around before energy depletion. In model B, the energy depletion somehow modifies the membrane structure. We have illustrated this change of membrane structure by moving other membrane proteins closer to the λ-receptor, and by making the attachment to the peptidoglycan layer stronger.

$$P_{\text{bead}}(f) \propto \left|\left\langle \tilde{x}_{\text{bead}}(f)\right\rangle\right|^2,$$

where $\tilde{x}_{\text{bead}}(f)$ is the Fourier-transform of positions, $x(t)$. The general result is

$$P_{\text{bead}}(f) = \frac{D_{\text{bead}}}{2\pi^2} \times \frac{(b+c)^2 + r^2(f/f_c)^2 + trb^2}{D}, \qquad (6)$$

with

$$D = f_c^2\left(r^2(f/f_c)^4 + \left((b+c)^2 + 2br^2 + r^2b\left(2+b^2\right)\right)\right.$$
$$\left.\times (f/f_c)^2 + \left(2bc(b+c) + (b+c)^2 + b^2c^2\right)\right) \qquad (7)$$

and where we have introduced the ratios

$$r = \frac{D_{\text{bead}}}{D_{\text{prot}}};\ b = \frac{\kappa_{\text{bs}}}{\kappa};\ c = \frac{\kappa_{\text{cw}}}{\kappa};\ f_c = \frac{\kappa}{2\pi\gamma_{\text{bead}}};\ t = \frac{T_{\text{bac}}}{T}. \qquad (8)$$

The way in which the general expression in Eq. 6 is fitted to experimental data depends upon which model is invoked, but in all cases, the data sets originating from metabolically competent and comprised cells are fitted simultaneously. In model A, $t = 1$ for the metabolically competent cells, but t is allowed to vary for the energy-depleted cells. In model B, κ_{cw} is allowed to have one value for the metabolically competent cells and another, $\kappa_{\text{cw,p}}$, for the energy-depleted (poisoned) cells. All other parameters are assumed identical for metabolically competent and comprised cells in the simultaneous fitting procedure.

RESULTS

Normal motion as revealed through quantum dot attachment

To determine the motility of a λ-receptor in a metabolically competent cell, we specifically attached a quantum dot to individual receptors. For each attached quantum dot, blinking was observed, which ensured that the signal originated from a single quantum dot. Analysis of time series of positions of individual quantum dots showed that a quantum dot attached to a λ-receptor always stays within a region of $\simeq 50$ nm. This is completely consistent with earlier results (4,5) as well as present results using micron-sized beads as handles. The remaining experiments of this work were done with 0.44-μm beads as handles, because these beads have the advantage over quantum dots that their motion can easily be monitored by the optical tweezers with superior temporal and spatial resolution, as compared to the image-based techniques.

Energy depletion

In all samples, the motion of the exact same λ-receptor was recorded before and after energy depletion. A time series showing the positions visited by the bead attached to the receptor before (*blue*) and after (*red*) energy depletion is shown in Fig. 2. The distributions of positions visited by an individual receptor, both before and after energy depletion are well fitted by Gaussian functions, shown as solid lines in the left inset of Fig. 2. The right inset of Fig. 2 shows a scatter plot of the positions visited before and after energy depletion. It is clear that the λ-receptor moves less after energy depletion. In total, 29 experiments were done, and they all showed a decrease in motility. This effect was also clearly visible by eye in the microscope, and it was observable immediately after the poisoning flushing procedure, which took a couple of minutes. I.e., the effect sets in rapidly, faster than 2 min.

This decrease of λ-receptor motility can be quantified by comparing the standard deviation of the position histograms (as shown in the *left inset* of Fig. 2) before and after energy depletion. For $n = 29$ data sets, we got $\sigma_{\text{before}} = (7.17 \pm 0.56)$ nm (mean ± SE) and $\sigma_{\text{after}} = (2.98 \pm 0.36)$ nm. To test whether these numbers are significantly different, a Student's t-test was performed. The p-value gives the probability that the observed difference between the two populations

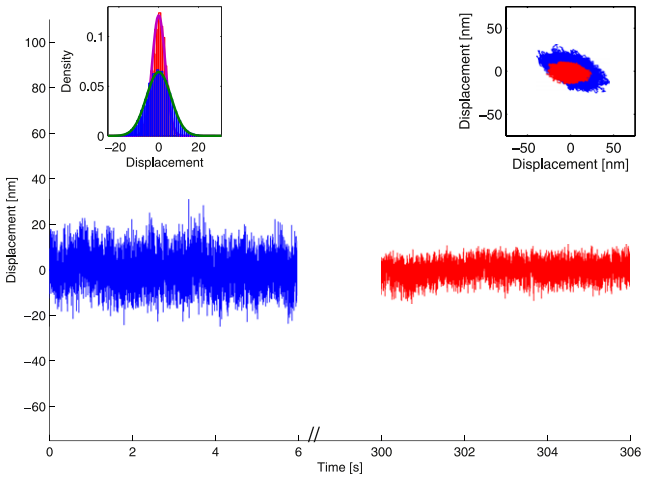

FIGURE 2 Effect of energy depletion. The graph shows the position as a function of time of a bead attached to a λ-receptor. The motility of the same receptor is shown both before (*blue*) and after (*red*) the energy poisoning by azide and arsenate. (*Left inset*) Histogram of the positions visited both before (*blue broad histogram*) and after (*red narrow histogram*) poisoning. (*Right inset*) Scatter plot of the positions visited by the bead-receptor complex both before (*blue*) and after (*red*) energy depletion.

is accidental. In other words, a low p-value supports the hypothesis of a significant change in motility upon energy depletion. The outcome of this analysis was $p = 3.6 \times 10^{-7}$. Hence, there is a significant change in motility of the λ-receptor upon energy depletion of the cell.

As a control, we investigated whether the exchange of media could be the cause of change of λ-receptor motility. The experiment mentioned above was repeated, but without azide and arsenate in the media which is flushed in. The result was that σ_{before} was not significantly different from σ_{after}. Hence, the observed change in motility was not simply an artifact of the flushing procedure.

The standard deviation of the bead, σ, gives clues about the motion of the bead linked to the receptor and hence, it indirectly provides information on the motion of the receptor itself. With the knowledge of κ and κ_{cw}, we used Eq. 4 to find σ_λ, the standard deviation of the motion of the λ-receptor without the effect of the optical trap. Using all the above-mentioned datasets, we found that for a normal metabolically competent cell, $\sigma_{\lambda,\ \text{before}} = (10.3 \pm 1.6)$ nm. For an energy-depleted cell, $\sigma_{\lambda,\ \text{after}} = (4.4 \pm 0.4)$ nm. A Student's t-test gives $p = 3.5 \times 10^{-4}$, in other words, the probability that the observed difference between the two populations is accidental is very low. Energy depletion of the cell causes a significant motility change for the λ-receptor.

For data acquisition, we used two different types of photodiodes, a quadrant photodiode (QPD) and a position-sensitive diode (PSD). Each photodiode has advantages and disadvantages, e.g., the quadrant photodiode has a pronounced filtering effect on frequencies above 10 kHz (24) but has a very low noise on the low-frequency part. The position-sensitive diode has a 3dB frequency that is somewhat larger than for the QPD, maybe at ~100 kHz, but it is a bit more noisy in the low-frequency regime. Hence, for the above-mentioned analysis of σ, both types of photodiodes could be employed, but for analysis of the power spectra, where the high-frequency regime is important, only the data acquired by the PSD could used. Fig. 3 shows a power-spectral analysis of one dataset acquired by the PSD. The upper set of data points originate from metabolically competent cells; the lower set originate from the same λ-receptor, but after energy depletion. Equation 6 stated in terms of model A (*solid lines* in Fig. 3) was simultaneously fit to both data sets. The inset shows the quality of the fit by dividing the data by the fit; ideally the distribution should be frequency independent, and one-third of the data points should be outside the two lines, each of which is located one standard deviation from 1.

Power-spectral analysis of all datasets acquired by the PSD allowed us to fit the data both by model A and model B. The outcome was that the χ^2 value from model A was smaller than that of model B in 10 out of 12 cases; in one case, the two values were indistinguishable. Fits of model A gave values for $\frac{T_{\text{bac}}}{T}$ and there seemed to be no dependence of this ratio on the stiffness of the optical trap (see Supporting Material). The average value was found as $\frac{T_{\text{bac}}}{T} = 10.5 \pm 3.8$. Fits of model B to the power spectral data sets gave values of $\frac{\kappa_{\text{cw,p}}}{\kappa_{\text{cw}}} = 27.6 \pm 12.4$ and again, there was no dependence of this ratio on the stiffness of the optical trap.

The ratios $\frac{T_{\text{bac}}}{T}$ and $\frac{\kappa_{\text{cw,p}}}{\kappa_{\text{cw}}}$ obtained from power-spectral analysis are equivalent to numbers which can be extracted from analysis of histograms as shown in the inset of Fig. 2. As evident from Eq. 3, the ratio $\frac{T_{\text{bac}}}{T}$ (model A) is equivalent to $\frac{\sigma^2_{\text{before}}}{\sigma^2_{\text{after}}}$. The values of $\frac{T_{\text{bac}}}{T}$ obtained from histogram analysis is also shown in the Supporting Material. From Eq. 4, it is evident that the ratio $\frac{\kappa_{\text{cw,p}}}{\kappa_{\text{cw}}}$ (model B) is equivalent to $\frac{\sigma^2_{\lambda,\text{before}}}{\sigma^2_{\lambda,\text{after}}}$.

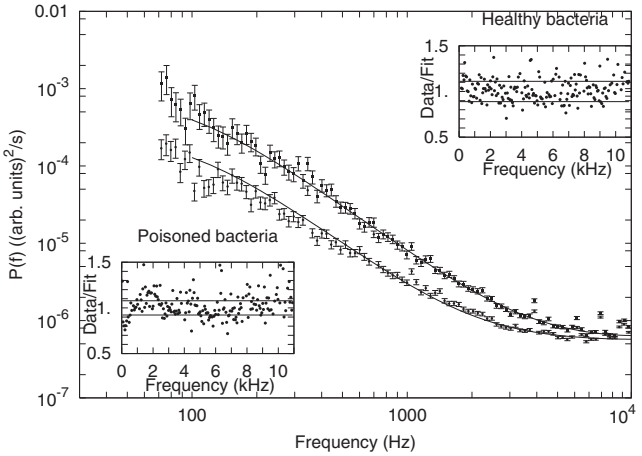

FIGURE 3 Power spectra calculated from the position time series of the λ-receptor before (*upper set* of *data points*) and after (*lower set* of *data points*) energy depletion. The solid lines overlaying the data show a fit of the model equation (Eq. 6) to the data, and the insets display scatter plots, demonstrating the quality of the fits. The data are fitted by model A.

The values of $\frac{T_{bac}}{T}$ and $\frac{\kappa_{cw,p}}{\kappa_{cw}}$ obtained by analyzing the histograms are in accordance with those obtained by power-spectral analysis (on a 5% significance level in a Student's *t*-test).

After treatment with ampicillin, we observed no change in cell shape. Therefore, damage to the cell wall was minor. Due to the length of time necessary to regenerate the cell wall after removal of ampicillin, we did not examine the same λ-receptor before and after regeneration. Instead, different populations were investigated. We had a population case 1, described in Materials and Methods, consisting of 38 datasets, which had been growing in ampicillin and where ampicillin was present during the preparation and measurement procedure; a population case 2, of 28 datasets which had been growing in ampicillin but where ampicillin was not present during the preparation and measurement procedure; and finally a control population case 3, consisting of 24 datasets without ampicillin but with all other parameters the same. Fig. 4 shows a time trace from a typical control cell (*blue*) and from a typical ampicillin-treated cell population 1 (*red*). There is a clear change in motility. This is also true if one considers all investigated cells: $\sigma_{control} = (11.32 \pm 0.89)$ nm and $\sigma_{ampicillin,\ case\ 1} = (3.43 \pm 0.32)$ nm. A Student's *t*-test gives a *p*-value of 2.1×10^{-14}. Hence, there is a very significant decrease in λ-receptor motility in cells treated and measured with ampicillin in comparison to the control. If, on the other hand, the cells were allowed to regenerate during the preparation and measurement procedure (which took ~1 h), it seemed that the λ-receptor could resume motion. The values quantifying the motility were $\sigma_{control} = (11.32 \pm 0.89)$ nm and $\sigma_{ampicillin,\ case\ 2} = (10.25 \pm 0.70)$ nm. A Students *t*-test gives a *p*-value of 0.11. Hence, the population cases 2 and 3 are not significantly different.

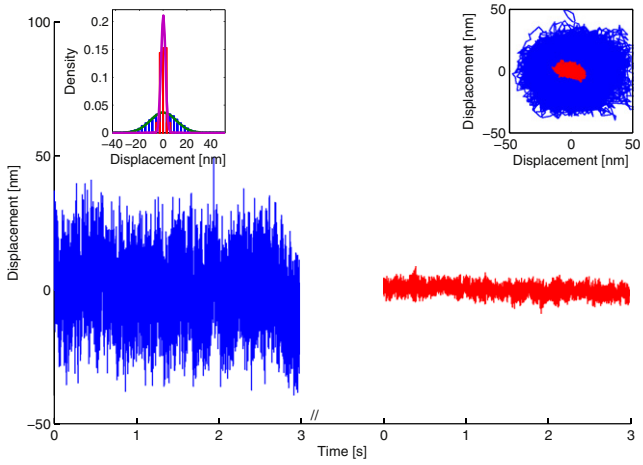

FIGURE 4 The effect of treating the cells with ampicillin. The graph shows the position as a function of time of a bead attached to a λ-receptor. The motility of a receptor is shown both with (*red*) and without (*blue*) treatment by ampicillin. (*Left inset*) Histogram of the positions visited both with (*red narrow histogram*) and without (*blue broad histogram*) ampicillin. (*Right inset*) Scatter plot of the positions visited both with (*red*) and without (*blue*) ampicillin.

DISCUSSION

In performing our analysis of the motility of λ-receptors in the outer membrane of *E. coli*, we utilize the inefficient conjugation of biotin to proteins exported from the cytoplasm (25,26). This allows us to limit the number of λ-receptors able to bind streptavidin to fewer than one per cell on average (4). In this and our previous studies (4,5), we found the λ-receptor diffused within a confined range of ~50 nm. Our previous analysis used only down to 0.44-μm streptavidin-coated spheres to visualize the movement of the biotinylated λ-receptors. It was hypothesized (6) that the large size of the spheres could hide a subpopulation with larger motility, as observed for a subset of λ-receptors monitored with 20-nm gold nanoparticles (6). To address this concern, we conducted single-particle tracking analysis using streptavidin-coated quantum dots. Using quantum dots 15 nm in diameter, we again observed diffusion limited to 50-nm domains, hence, the size of the handle cannot be the cause. Due to inefficient biotinylation, the strains used in this investigation and in the literature (4,5) had, on average, less than one binding site per bacterium. This is important because it increases the likelihood of having only a single λ-receptor attached to the probe particle. Usually only a single probe particle attached itself per bacterium, which minimizes the risk of overlaying motility trajectories from adjacent probe particles. The strains used in Gibbs et al. (6) had all λ-receptors expressing gold-binding sites, hence, potentially the 20-nm gold nanobeads could bind to hundreds or thousands of λ-receptors available on a single bacterium. Because the point-spread function of a 20-nm gold nanoparticle is ~300 nm, two or more particles closer than 300 nm would appear as one point when imaged by light microscopy. A centroid tracking routine utilizes the picture from the microscope; although it can reliably track one particle with a resolution down to 10 nm, it is not able to track the centroid of a particle if its point-spread function overlaps with those of other particles. Therefore, we suggest that the subpopulation of λ-receptors observed in Gibbs et al. (6), postulated to move distances of 300 nm, could be an artifact caused by two or more gold nanoparticles with trajectories located within each other's point-spread function.

Upon energy depletion of the cells by azide and arsenate, there was a significant decrease of motility of the λ-receptor. The change in motility occurred rapidly, on a timescale faster than minutes. One of the actions of azide is to block electron transport. In the absence of phosphate, arsenate blocks ATP synthesis. Hence, with these two poisons the cells had their energy metabolism effectively stopped. There have been theoretical reports predicting a correlation between protein motility and the energetic state of the membrane (i.e., (8,27)). However, to our knowledge, the effect of energy on the motility of membrane proteins has not been observed before. The fact that we clearly see a connection between the energetic state of the bacterium and the motility of the

λ-receptor signifies, first of all, that the bacterium uses energy to move the λ-receptor. A highly energetically optimized system as a bacterium would never waste its energy, therefore there must be a benefit to this motion. Secondly, the fact that the λ-receptor moves more in a metabolically competent cell than in an energy-depleted cell at the same temperature means that its motion cannot be attributed to thermal fluctuations alone. Our observations of energy dependence in the movement of the λ-receptor should be considered when comparing diffusion in artificial membranes to diffusion in the membranes of living bacterial cells.

To elucidate the cause of the observed decrease of λ-receptor motility we invoked two models. The first, model A, assumed that the change in motility was caused by some ATP-based activation energy that the bacterium uses to wiggle its λ-receptor when it is in a metabolically competent state. A fit of model A to the data showed that this activation energy, E_{active} from Eq. 5, should be approximately nine times larger than the thermal energy of the λ-receptor. The second, Model B, assumed that the observed decrease of λ-receptor motility was caused by a change in the stiffness of the attachment between the λ-receptor and the cell wall, κ_{cw}. A fit of model B to the data revealed that κ_{cw} should increase by a factor of ~28 upon energy depletion. The biological causes of such a stiffening could, for instance, be an aggregation of proteins around the λ-receptor, a stiffening of the lipids in the membrane, or a stiffening of the peptidoglycan layer, to which the λ-receptor is assumed attached (12). A χ^2 test of the two models is in favor of model A. However, in reality, the reduced motility is probably influenced by a mixture of both mechanisms. For convergence reasons, it was not possible to let too many parameters flow in the data analysis and we had to make separate fits of models A and B to the data.

To shed more light on the biological cause of the wiggling motion of the λ-receptor, we also performed experiments where the peptidoglycan was damaged by ampicillin, a common antibiotic. Ampicillin hinders crosslinking of peptide bonds in the peptidoglycan layer and hence, inhibits the constant dynamic remodeling of the peptidoglycan layer. The result of ampicillin treatment was to efficiently stop the motion of the λ-receptor. However, if the cells were allowed to revive without ampicillin present, the receptors resumed the same motility as in the untreated cells. The decrease in motility upon ampicillin treatment is consistent with the results from Gabay and Yasunaka (12), where the λ-receptor is postulated to be attached to the peptidoglycan, firmly enough to withstand sodium dodecyl sulfate treatment. The fact that the λ-receptor resumes its motion upon removal of ampicillin suggests that the motility of the λ-receptor is very closely linked to the dynamic reconstruction of the peptidoglycan layer. ATP is not readily available within the periplasm, which also supports the idea that an active ATP-dependent motion must be coupled to processes occurring other places, e.g., in the peptidoglycan layer.

Why would a bacterium spend energy moving its λ-receptor in the membrane? As the role of the λ-receptor is to facilitate the diffusion of maltodextrins across the outer membrane of Gram-negative bacteria, it is likely that the observed motility assists this task. It has been shown by crystallography that the λ-receptor has a so-called ''greasy slide'' consisting of six contingent aromatic residues, to which maltooligosaccharide binds during its guided diffusion into the cell (28,29). We suggest that the motility of the receptor, the wiggling motion (4,6), assists in the guided diffusion, maybe by shaking the polymer loose from the greasy slide—an effect somehow parallel to the shaking of a salt container to overcome compactification of the salt crystals such that gravity can force salt onto your plate. The parallel of gravity would be the electrochemical potential favoring a cytoplasmatic position of the polymer. We suggest that the binding of the λ-receptor to the peptidoglycan layer is a convenient way to make the receptor actively move; the natural and constant reconstruction of the peptidoglycan will simply make anything connected to it move as well. When the cell is depleted of energy (e.g., by azide and arsenate poisoning), this energy-consuming reconstruction of the peptidoglycan can no longer take place and the λ-receptor stops moving. Another way to stop the motion is to directly target the peptidoglycan by ampicillin, which has a similar effect.

The λ-receptor also serves as the receptor for phage-λ, and it is a possibility that this active wiggling motion also could somehow influence the injection of λ-DNA. However, as even purified λ-receptors can cause release of λ-DNA from the phage (30), phage infection is not crucially dependent upon this wiggling motion.

Future investigations will include observations of motility of other bacterial outer membrane proteins, among which are some that are known not to link to the peptidoglycan layer, and we will investigate the effect of drugs that target structures other than the peptidoglycan layer. In addition, it is an interesting question whether a similar effect is present in eukaryotic cells with a very different membrane structure.

CONCLUSION

We investigated the motility of a single λ-receptor in the outer membrane of *E. coli* and the dependence on energy metabolism. In an energetically competent cell, experiments using quantum dots as markers showed, in accordance with part of earlier literature (4,5), that all λ-receptors performed a confined diffusion with a typical range of 50 nm. Poisoning the cell by azide and arsenate, which stops energy metabolism, causes a rapid and significant decrease of motion of the λ-receptor. We propose a model with two possible causes of this decreased motility in energy-depleted cells. One possible cause could be that an energetically competent cell actively uses energy to move the λ-receptor; this energy would be approximately one-order-of-magnitude larger than

thermal energy. Another cause could be that the attachment between the λ-receptor and the membrane structure changes, e.g., by an aggregation of proteins or a stiffening of some part of the membrane structure. To further pinpoint the biological cause of the observed decreased motility, the effect of ampicillin treatment was investigated. Ampicillin directly targets the peptidoglycan layer, hindering transpeptidase action. Ampicillin effectively stopped the motility of the λ-receptor but we also observed that this effect was reversible. In summary, we propose that the λ-receptor is linked to the peptidoglycan layer and that the observed motility of the λ-receptor is directly linked to the energy-dependent dynamic reconstruction of the peptidoglycan layer.

SUPPORTING MATERIAL

One figure is available at http://www.biophysj.org/biophysj/supplemental/S0006-3495(09)01161-8.

We are very grateful for discussions with T. Silhavy, K. Sneppen, R. Lipowsky, and T. Heimburg. We deeply appreciate help from L. Jauffred with the quantum dot experiments.

REFERENCES

1. Nakada, C., K. Ritchie, Y. Oba, M. Nakamura, Y. Hotta, et al. 2003. Accumulation of anchored proteins forms membrane diffusion barriers during neuronal polarization. *Nat. Cell Biol.* 5:626–632.
2. Suzuki, K., K. Ritchie, E. Kajikawa, T. Fujiwara, and A. Kusumi. 2005. Rapid hop diffusion of a G-protein-coupled receptor in the plasma membrane as revealed by single-molecule techniques. *Biophys. J.* 88:3659–3680.
3. Ritchie, K., and J. Spector. 2007. Single molecule studies of molecular diffusion in cellular membranes: determining membrane structure. *Biopolymers.* 87:95–101.
4. Oddershede, L., J. Dreyer, S. Grego, S. Brown, and K. Berg-Sørensen. 2002. The motion of a single molecule, the λ-receptor, in the bacterial outer membrane. *Biophys. J.* 83:3152–3161.
5. Oddershede, L., H. Flyvbjerg, and K. Berg-Sørensen. 2003. Single-molecule experiment with optical tweezer improved analysis of the diffusion of the λ-receptor in *E. coli*'s outer membrane. *J. Phys. Condens. Matter.* 15:S1737–S1746.
6. Gibbs, K., D. D. Isaac, J. Xu, R. W. Hendrix, T. J. Silhavy, et al. 2004. Complex spatial distribution and dynamics of an abundant *Escherichia coli* outer membrane protein, LamB. *Mol. Microbiol.* 53:1771–1783.
7. de Pedro, M., C. Grunfelder, and H. Schwarz. 2004. Restricted mobility of cell surface proteins in the polar regions of *Escherichia coli*. *J. Bacteriol.* 1:2594–2602.
8. Sabra, M., and O. Mouritsen. 1998. Steady-state compartmentalization of lipid membranes by active proteins. *Biophys. J.* 74:745–752.
9. Kaya, N., D. Wiersma, B. Poolman, and D. Hoekstra. 2002. Spatial organization of bacteriorhodopsin in model membranes. *J. Biol. Chem.* 277:39304–39311.
10. Nikaido, H. 2003. Molecular basis of bacterial outer membrane permeability revisited. *Microbiol. Mol. Biol. Rev.* 67:593–656.
11. Szmelcman, S., and M. Hofnung. 1975. Maltose transport in *Escherichia coli* K-12: involvement of the bacteriophage lambda receptor. *J. Bacteriol.* 124:112–118.
12. Gabay, J., and K. Yasunaka. 1980. Interaction of the *lamB* protein with the peptidoglycan layer in *Escherichia coli* K12. *Eur. J. Biochem.* 104:13–18.
13. Ryter, A., H. Shuman, and M. Schwartz. 1975. Integration of the receptor for bacteriophage lambda in the outer membrane of *Escherichia coli*: coupling with cell division. *J. Bacteriol.* 122:295–301.
14. Vos-Scheperkeuter, G., E. Pas, G. Brakenhoff, N. Nanninga, and B. Witholt. 1984. Topography of the insertion of LamB protein into the outer membrane of *Escherichia coli* wild-type and lac-lamB cells. *J. Bacteriol.* 159:440–447.
15. Ghosh, A., and K. Young. 2005. Helical disposition of proteins and lipopolysaccharide in the outer membrane of *Escherichia coli*. *J. Bacteriol.* 187:1913–1922.
16. Brown, S. 1997. Metal-recognition by repeating polypeptides. *Nat. Biotechnol.* 15:269–272.
17. Miller, J. 1972. Experiments in Molecular Genetics. Cold Spring Harbor Laboratory Press, New York.
18. Pardee, A., F. Jacob, and J. Monod. 1959. The genetic control and cytoplasmic expression of "inducibility" in the synthesis of β-galactosidase by *E. coli*. *J. Mol. Biol.* 1:165–178.
19. Neidhardt, F., P. Bloch, and D. Smith. 1974. Culture medium for enterobacteria. *J. Bacteriol.* 119:736–747.
20. Oddershede, L., S. Grego, S. Nørrelykke, and K. Berg-Sørensen. 2001. Optical tweezers: probing biological surfaces. *Probe Microsc.* 2:129–137.
21. Rasmussen, M., L. Oddershede, and H. Siegumfeldt. 2008. Optical tweezers cause physiological damage to *E. coli* and *Listeria* bacteria. *Appl. Environ. Microbiol.* 74:2441–2446.
22. Jauffred, L., T. Callisen, and L. Oddershede. 2007. Viscoelasticity of bacterial tethers. *Biophys. J.* 93:1–8.
23. Hansen, P., I. Tolic-Nørrelykke, H. Flyvbjerg, and K. Berg-Sørensen. 2006. Tweezercalib 2.0: faster version of a MatLab package for precision calibration of optical tweezers. *Comput. Phys. Commun.* 174: 518–520.
24. Berg-Sørensen, K., L. Oddershede, E.-L. Florin, and H. Flyvbjerg. 2003. Unintended filtering in typical photodiode detection system for optical tweezers. *J. Appl. Phys.* 93:3167–3176.
25. Reed, K., and J. J. E. Cronan. 1991. *Escherichia coli* exports previously folded and biotinylated protein domains. *J. Biol. Chem.* 266:11425–11428.
26. Jander, G., J. J. E. Cronan, and J. Beckwith. 1996. Biotinylation in vivo as a sensitive indicator of protein secretion and membrane protein insertion. *J. Bacteriol.* 178:3049–3058.
27. Gov, N. 2004. Membrane undulations driven by force fluctuations of active proteins. *Phys. Rev. Lett.* 93:1–4.
28. Schirmer, T., T. Keller, Y.-F. Wang, and J. Rosenbusch. 1995. Structural basis for sugar translocation through maltoposin channels at 3.1 Å resolution. *Science.* 267:512–514.
29. van Gelder, P., F. Dumas, I. Bartoldus, N. Saint, A. Prilipov, et al. 2002. Sugar transport through maltoporin of *Escherichia coli*: role of the greasy slide. *J. Bacteriol.* 184:2994–2999.
30. Randall-Hazelbauer, L., and M. Schwartz. 1973. Isolation of the bacteriophage lambda receptor from *Escherichia coli*. *J. Bacteriol.* 116:1436–1446.